Particle Accelerators
1980, Vol. 11, pp. 1-13
0031-2460/80/1101-0001 $06.50/0

BEAM OPTICAL CONTROL OF BEAM BREAKUP IN A RECIRCULATING ELECTRON ACCELERATOR*

R.E. RAND AND T.I. SMITH

High Energy Physics Laboratory, Stanford University, Stanford, California 94305 U.S.A.

(Received June 27, 1979)

The relationship of regenerative beam breakup (BBU) in a recirculating electron accelerator (recyclotron or microtron) to the orbital beam optics is discussed. To reduce BBU, the optics should be designed so that deflection of the beam during a given traversal of the structure produces minimum displacement of the beam during subsequent traversals. The selection of orbit matrices to achieve this result is discussed. Implications of these calculations for the magnitudes of the BBU starting currents are illustrated using experimental data from the Stanford superconducting recyclotron. It is shown that in principle BBU can be suppressed completely in the first orbit by "reflection" or "rotation" of the beam.

INTRODUCTION

High duty-factor, high-current (and high-beam quality) electron accelerators are currently being considered for the next generation of electron-scattering experiments, which will investigate nuclear structure by coincidence techniques.[1] The only method available at present of accelerating electrons with high current and high duty factor is by means of a linac, either superconducting[2] or conventional.[3] High duty factor necessitates low energy gradients in both cases, so that for final energies of several hundred MeV, the length becomes prohibitive. Hence machines are being built and proposed where the beam is recirculated through the linac many times. These machines fall into two main types, the recyclotron,[2] and the race-track microtron.[4]

The beam current which may be accelerated by these accelerators is limited by a regenerative beam breakup (BBU) phenomenon that is rather different from that encountered in a linac. This BBU arises because of the interaction of the recirculated beams with the TM_{11} deflecting modes of the accelerating structures.[5] In superconducting structures, these modes can have Q values of order 10^9 and if not loaded down, will restrict average recirculated currents to the order of 0.1 to 10 μA.[2,4] Even room-temperature accelerators such as the proposed microtron at Mainz[6] are expected to be limited to currents of approximately 16 μA by this effect.

Although this phenomenon may be suppressed by loading the transverse modes of the cavities with resistive probes, this alone is not necessarily sufficient to produce acceptable BBU starting currents. The purpose of this paper is to point out that careful selection of orbit beam optics is also an essential part of the design which can enhance performance significantly.

*Work supported by the National Science Foundation under Grant #PHY79-05286.

2 BEAM OPTICAL CONTROL OF BEAM BREAKUP

The general principle of beam optical control will be illustrated by assuming initially that all deflections and displacements of the beam are confined to one plane, for instance, the bending or x-plane. Consider the first orbit of recirculation. The first-pass beam may be perturbed by the transverse magnetic fields of a potential BBU mode. This can lead in turn to a displacement of the second (or higher) pass beam, which may feed energy into the mode by interaction with its longitudinal electric fields. If this energy is supplied faster than the rate at which the mode decays, BBU occurs.

The perturbation of the primary beam is dominated by deflection, although if the phase slip of the beam with respect to the BBU mode during the first pass is not zero, a displacement of the beam is also possible. For a transverse field that could cause an intolerable deflection of the beam, the order of magnitude of the possible displacement is much less than the typical beam size. Hence deflections of the primary beam are generally most important.

The BBU modes are of a dipole nature, so that for a given field amplitude the rate at which energy is fed into the mode is proportional to the displacement of the second-pass beam. Hence it can be shown that

the starting current for BBU is proportional to the energy E_A (strictly momentum) of the first-pass beam and inversely proportional to the displacement of the centroid of the beam at second pass, due to unit deflection during the first pass, i.e., the magnitude of the "orbit matrix" element R_{12}, in TRANSPORT[7] notation.[8] (The "orbit matrix" is defined as the beam-transport matrix from a given point in the linac back to the same point at the subsequent pass.)

Thus the obvious strategy for reducing BBU is to minimize $|R_{12}|/E_A$ as much as possible for all points in the linac. This is a general technique that is applicable to all orbits. There are certain special techniques which apply only to the first orbit. These will be mentioned later.

BBU also depends of course on the phase shift of the beam around the orbit at the frequency of the breakup mode. A study of this dependence has been made by Vetter et al.[5]

3. CHOICE OF ORBIT MATRIX

3.1 Point-to-point Focusing

The ideal condition for minimizing BBU is point-to-point focusing in both planes, i.e., $R_{12} = R_{34} = 0$, at all points in the linac. In general, this condition cannot be satisfied exactly except in the limit of no acceleration. As will be seen below, the best approximation to this ideal that can be achieved in practice is $R_{12} = R_{34} = 0$ at three points in the linac.

It is convenient to investigate the optimization of the first-orbit optics by assuming that the orbit matrix is arranged so that $R_{12} = R_{34} = 0$ at a point, whose distance from the injection end of the linac is L_p. It will be assumed that there is no mixing between the x- and y-planes. The first-order orbit matrix at L_p in either plane is then of the form

$$R_p = \begin{bmatrix} M & 0 \\ C & X_p/M \end{bmatrix}, \tag{1}$$

where M is the magnification around the orbit, C represents R_{21} or R_{43}, $X_p = E_A/E_B$ and E_A, E_B are respectively the energies of the first- and second-pass beams at L_p (see Fig. 1).

Now consider a point in the linac a distance L downstream from L_p. The orbit matrix at this point may be written $R = \alpha_B(L)R_p\alpha_A^{-1}(L)$, where $\alpha_A(L)$, $\alpha_B(L)$ are the transport matrices for the linac from L_p to $(L_p + L)$ for the primary and second-pass beams respectively. Using matrices for standing[9]- and traveling[7]-wave structures, the quantity $R_{12}/(E_A + E)$, where E is the energy gain corresponding to the length L, has been calculated. Complete results are given here for standing-wave structures, since these are directly applicable to the Stanford superconducting linac. Corresponding results for the traveling-wave case are given in the appendix.

The TRANSPORT matrix for a standing-wave structure (for an integral number of periods) is of the form (with symbols as defined in Fig. 1).

$$\alpha_A(L) = \begin{bmatrix} C_A - \tfrac{1}{2}S_A & L_A S_A \\ -\tfrac{3}{8}\dfrac{X_A}{L_A}S_A & X_A(C_A + \tfrac{1}{2}S_A) \end{bmatrix},$$

where $S_A = (8)^{1/2} \sin A$, $C_A = \cos A$, $A = (1/\sqrt{8}) \ln (1/X_A)$, and $X_A = L_A/(L_A + L)$. $\alpha_B(L)$ is similarly defined.

Hence

$$\frac{R_{12}}{E_A + E} = \frac{L_0}{E_0}\left[\frac{1}{M} S_B(C_A - \tfrac{1}{2}S_A) - MS_A(C_B - \tfrac{1}{2}S_B) - \frac{E_A}{E_0 X_p} CL_0 S_A S_B\right]. \tag{3}$$

By choosing M and C appropriately, one can set $R_{12}/(E_A + E) = 0$ at two values of L, say L_1 and L_2, as well as at $L = 0$. [The trigonometric functions involved in $R_{12}/(E_A + E)$ span only a fraction of a period in all practical cases.] The necessary magnification is then determined by

$$M^2 = \frac{S_{B1}S_{B2}(S_{A2}C_{A1} - S_{A1}C_{A2})}{S_{A1}S_{A2}(S_{B2}C_{B1} - S_{B1}C_{B2})}, \tag{4}$$

which always has real roots such that $M \simeq \pm\sqrt{X_p}$.

Some insight into the exact expression (3) for $R_{12}/(E_A + E)$ may be gained by expanding R_{12} as a power series in L, i.e.,

$$R_{12} = L\left[\frac{X_p}{M} - M\right] + \frac{L^2}{L_0}\left[\frac{E_0}{2E_A}(1 - X_p) \times \left(\frac{X_p}{M} - M\right) - CL_0\right] + \frac{L^3}{L_0^2}\left[-\left(\frac{E_0}{2E_A}\right)^2\right.$$

$$\times X_p\left(\frac{X_p}{M} - M\right) - \tfrac{1}{4}\left(\frac{E_0}{2E_A}\right)^2 (1 - X_p^2)$$
$$\times\left(\frac{5X_p}{M} - 3M\right) - \frac{E_0}{2E_A}\,(1 - X_p)\,CL_0\Big] + \ldots\ldots \quad (5)$$

This third-order expression is surprisingly accurate even for small E_A/E_0, as will be shown below.

The problem now is to find the values of L_p, M and C that minimize $|R_{12}|/(E_A + E)$ for all points in the linac. This requirement is interpreted throughout this paper to mean that the extreme values of $|R_{12}|/(E_A + E)$ should be minimized, although when phase and other effects are taken into account, this is not necessarily the optimum condition.

An approximate analytical solution to the optimization problem is available only for the case $E_A \gg E_0$. This is most useful for high injection energy or higher orbits of recirculation. In this case, the maxima of $|R_{12}|/(E_A + E)$ are at the maxima of $|R_{12}|$.

Therefore by symmetry $L_p \simeq \frac{1}{2} L_0$ and the requirement that the coefficient of L^2 be equal to zero, determines CL_0 in terms of M. Furthermore it is necessary to have $R_{12} = 0$ close to the ends of the linac, i.e., $L_1 \simeq -\frac{1}{2} L_0$, $L_2 \simeq \frac{1}{2} L_0$. Hence it can be shown that the maxima of $|R_{12}|$ occur at $L \simeq \pm L_0/2\sqrt{3}$ where $R_{12} = \pm L_0[(X_p/M) - M]/3\sqrt{3}$.

Other quantities of interest are

$$M^2 \simeq X_p\left[1 - \tfrac{1}{8}\left(\frac{E_0}{2E_A}\right)^2 (1 - X_p^2)\right], \quad (6)$$

$$CL_0 \simeq \tfrac{1}{8}\left(\frac{E_0}{2E_A}\right)^3 (1 - X_p^2)(1 - X_p)\sqrt{X_p}, \quad (7)$$

and

$$\left(\frac{|R_{12}|}{E_A + E}\right)_{\max} \simeq \frac{L_0}{12\sqrt{3}\,E_0}\left(\frac{E_0}{2E_A}\right)^3 \times (1 - X_p^2)\sqrt{X_p}. \quad (8)$$

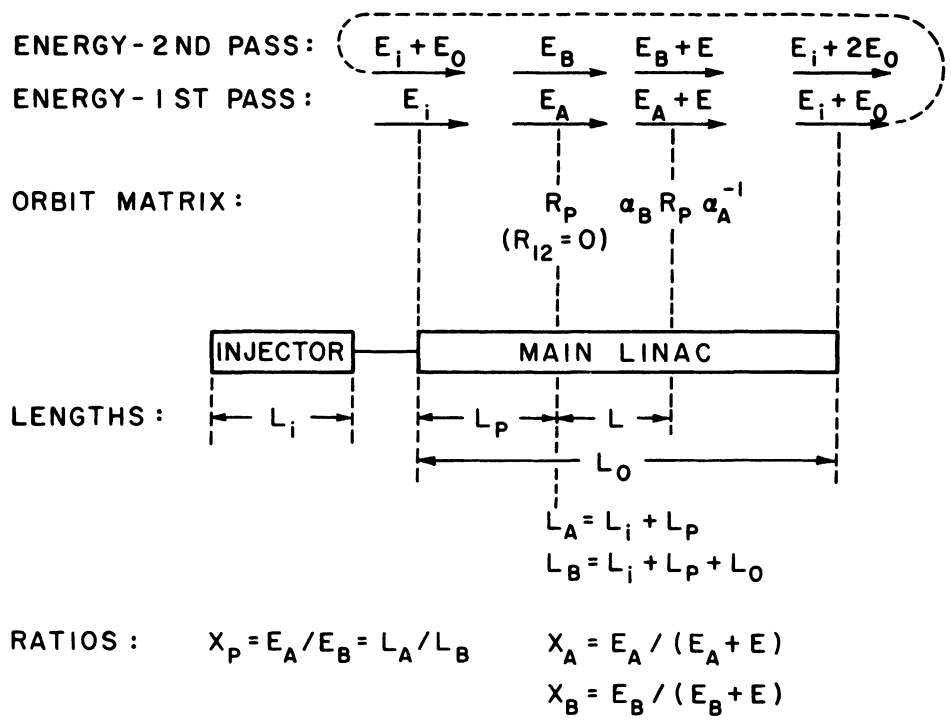

FIGURE 1 Defintion of symbols—first orbit.

In the limit of negligible energy gain per pass, the required orbit parameters become $M^2 \simeq X_p$ and $C L_0 \simeq 0$, i.e., a diagonal orbit matrix with $R_{12} \simeq 0$ for all points in the linac. Examples of ray diagrams for diagonal orbit matrices are shown in Fig. 2.

The optimization problem cannot be solved analytically for low injection energy, but a good approximation to L_p may be obtained by assuming $M^2 = X_p$, $C = 0$, and calculating from the third-order expression (5) the condition for equal $|R_{12}|/(E_A + E)$ at the ends of the linac. This gives

$$L_p \simeq L_0 [1 + (1 + E_0/E_i)^{1/3}]^{-1}. \quad (9)$$

For the numerical example considered below, this expression proves to be quite adequate.

We now come to the problem of matrix optimization for multiple orbits. (All formulae given above are valid for any group of consecutive orbits if E_A and E_B are respectively replaced by the energies of the beam at the first and last passes defining the group.) Consider the displacement of the centroid of the beam in pass N due to deflections suffered during all previous passes. In general it is most important to minimize the extreme values of $R^{AN}_{12}/(E_A + E)$ where R^{AN}_{12} is an element of the transport matrix from pass A to pass N. Next in order of importance would be to minimize the quantity $R^{BN}_{12}/(E_B + E)$, but as expression (8) shows, this is already a factor $(E_B/E_A)^{5/2}$ less significant than the equivalent first-pass quantity. Hence perturbation of the first-pass beam is the dominant effect.

It is expedient to think in terms of the third-order approximation (5) for R^{AN}_{12}. The shape of the curve $R^{AN}_{12}/(E_A + E)$ may be described by three parameters L_p, L_1 and L_2, which define the positions where $R^{AN}_{12} = 0$. The optimum values of these parameters depend only on the ratio of injection energy to energy gain per pass. Hence for different N, $R^{AN}_{12}/(E_A + E)$ differs only by a scaling factor and the corresponding magnification M^{AN} and matrix parameter C^{AN} may be calculated from the previous formulae with subscript N substituted for B.

It is interesting to note that the exact expression (4) for optimum magnification can be cast in the form

$$M^{AN} = \frac{f(A)}{f(N)} = \frac{f(A)}{f(B)} \times \frac{f(B)}{f(C)} \times \ldots \times \frac{f(M)}{f(N)}. \quad (10)$$

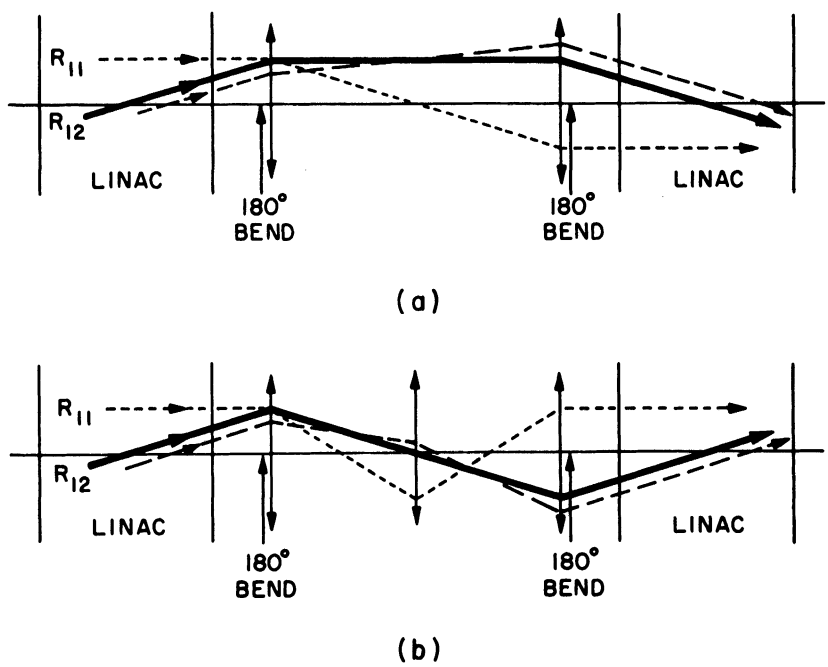

FIGURE 2 Diagonal matrix orbit optics for a recyclotron with (a) negative magnification (b) positive magnification in the limit of no acceleration. Each lens is a quadrupole pair. Optical effects (inversion) at the 180° bends in the bend plane have been ignored.

Thus the condition for $R_{12} = 0$ at the same L_p, L_1 and L_2 for each orbit individually is consistent with the overall requirement. A similar statement is true for the orbit matrix parameter C^{AN}, but the functional dependence is more complicated.

The signs of the orbit magnifications also influence BBU for multiple orbits. For instance, consider the first two orbits. At an arbitrary point in the linac, $R^{AC}_{12} \simeq M^{AB} R^{BC}_{12} + M^{BC} R^{AB}_{12} \simeq M^{BC} R^{AB}_{12}$. Now energy may be fed into the BBU mode by both the second- and third-pass beams. Therefore the starting current for BBU becomes inversely proportional to $R^{AB}_{12}(1 + pM^{BC})$, where p depends on the orbital phase shifts. The optimum sign for M^{BC} then depends on the frequency of the dominant BBU mode.

For the first orbit, numerical calculations are generally necessary to find the optimum values of L_p, M and C. For the orbit matrix starting at L_p, these define six independent conditions: $R_{11} = R_{33} = M$; $R_{12} = R_{34} = 0$, $R_{21} = R_{43} = C$. The recirculation system should be sufficiently flexible that any such given set of conditions can be attained. For instance the orbits of the Stanford superconducting recyclotron[2] (SCR) each have at least six quadrupoles, so that in general a solution is possible. Such solutions may be found using a program such as TRANSPORT.

To demonstrate the orders of magnitude involved in the above theory and to give one example of orbit optimization, sample calculations have been made with $E_i/E_0 = 0.2$.

Figure 3 shows exact calculations made with the approximate value of L_p for high injection energy; $L_p = \frac{1}{2} L_0$. Here $R_{12}/(E_A + E)$ and R_{12} are plotted in a non-dimensional form for the case where $R_{12} = 0$ at both ends of the linac. The third-order approximation *(5) to* R_{12} is also shown for the same boundary conditions. For most purposes this approximation would be adequate. In this case the maximum value of $E_0|R_{12}|/L_0(E_A + E)$ is ~ 0.028 near the injection end of the linac.

An attempt at minimizing the extreme values of $|R_{12}|/(E_A + E)$ is shown in Fig. 4. Here L_p has been calculated from equation (9). For this value of L_p, three sets of curves have been calculated. These are (a) $R_{12} = 0$ at both ends of the linac, (b) $M = (X_p)^{1/2}$, $C = 0$(diagonal matrix), and (c) optimum conditions. In the second case, the third-order

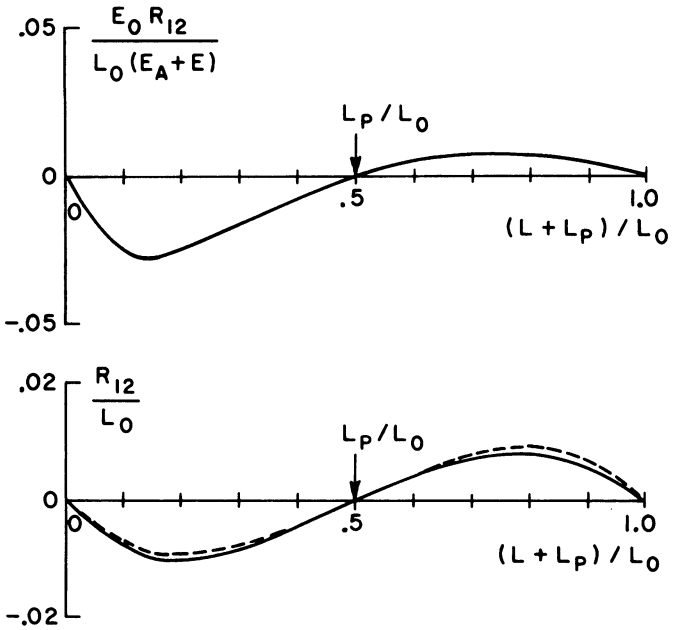

FIGURE 3 Calculated values of $E_0\ R_{12}/L_0(E_A + E)$ and R_{12}/L_0 for $E_i/E_0 = 0.2$, $L_p/L_0 = 0.5$. Curves are fitted to $R_{12} = 0$ at both ends of the linac: $M = 0.61919$, $CL_0 = 0.0395$. Solid lines—exact calculation, dashed line—third order approximation.

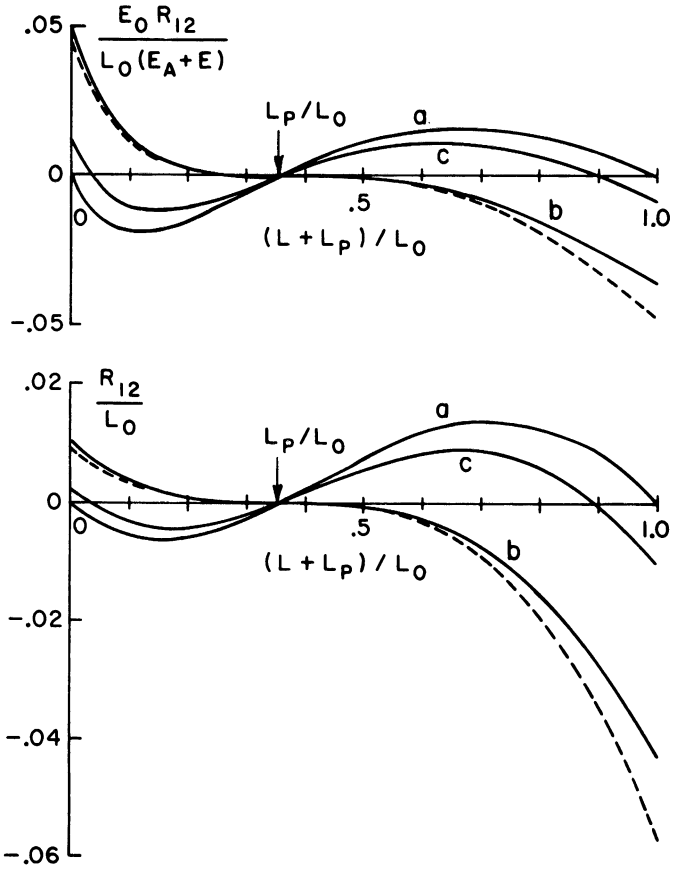

FIGURE 4 Calculated values of $E_0\ R_{12}/L_0(E_A + E)$ and R_{12}/L_0 for $E_i/E_0 = 0.2$, $L_p/L_0 = 0.355$.
curves (a): $R_{12} = 0$ at both ends of linac: $M = 0.57255$, $C\ L_0 = -0.0314$
curves (b): Diagonal orbit matrix: $M = 0.59742$, $C\ L_0 = 0$
curves (c): Extreme values of $E_0|\ R_{12}|\ /L_0(E_A + E)$ minimized: $M = 0.5784$, $C\ L_0 = -0.010$
Solid lines—exact calculation, dashed lines—third order approximation.

approximation is also shown for comparison. The optimum curve (c) shows that the approximate value for L_p is not quite correct, but certainly acceptable. The minimized value for the extremes of $E_0|\ R_{12}|\ /L_0(E_A + E)$ is ~ 0.11.

3.2. Experimental Tests

To illustrate the quantitative implications of these calculations with respect to BBU starting currents, measurements of the latter have been made under known beam optical conditions on the Stanford SCR. This machine consists at present of 3 superconducting standing-wave structures, each of length 6 m. The optics of each orbit of recirculation may be varied by 3 pairs of quadrupoles. The final design allows for 8 accelerator structures and 4 orbits of recirculation. The tests were made with an injection energy of 5 MeV and an energy gain per pass of 36.5 MeV for 2- and 3-pass operation. The behavior of the SCR was observed with a central accelerating structure whose transverse modes were not damped and which in fact had Q values of order 10^9. These Q values have subsequently been reduced to the order of 10^7 to 10^8 by inserting appropriate resistive probes. The transverse modes in the other structures

were already loaded down to this level. This discussion ignores the effect of the phase shift of the beam at the frequencies of the transverse modes.

For the first orbit, for an arbitrary non-point-to-point orbit matrix, it is common to observe BBU starting currents as low as 0.5 μA (average). For a point-to-point configuration with $M_x = 0.16$ and $M_y = 0.30$, implying $R_{12}/L = 1.92$ and $R_{34}/L = 0.81$ [only the first-order terms in L are significant in equation (5)], the BBU starting current was observed to be approximately 2 μA. For a second configuration with $M_x = -0.44$, $M_y = 0.51$, $R_{12}/L = -0.32$ and $R_{34}/L = 0.14$ and the same energy the starting current was approximately 12 μA. These results imply that BBU was due to a mode which deflects the beam almost vertically. The plane of deflection was actually observed to be oriented at about 60° to the horizontal.

Although BBU actually occurred in the non-damped accelerating structure, the significant result for the eventual configuration of the machine was that it did not occur in the first loaded structure, where it is estimated $E_0 |R_{12}| / L_0(E_A + E) = 2.6$. With careful orbit design, this quantity can be reduced by up to two orders of magnitude. Therefore in the final configuration, it is possible that the starting current for BBU in the first orbit could be as high as 1 mA.

Tests with a 3-pass beam showed a BBU starting current of 3.6 μA, with a magnification for the second orbit of + 0.8 in both planes. Disregarding the different phase shifts for the two orbits, one would naively expect in this case a starting current of $12/1.8 \simeq 7$ μA, showing that the phase-shift effect is significant.

3.3 Beam Reflection

The discussion so far has assumed that there is no mixing between the horizontal and vertical plane of the orbit optics or, equivalently, that the breakup modes are polarized in these planes. In the more general case of orthogonal transverse structure modes oriented at angles β and (90° + β) to the horizontal plane, a further increase in BBU starting current can be obtained by using a "reflector" or "mirror" configuration for the first-orbit matrix.

A reflector configuration is defined as one in which R_{12} and R_{34} are of opposite sign. This can generally be achieved with magnifications of opposite sign although, as formulae (3) and (5) show, there are other possibilities.

To see how this can be useful for increasing BBU starting currents, suppose that a displacement $\mathbf{r}$ of the second-pass beam is caused by a deflection $\mathbf{r}'_0 = (x'_0, y'_0)$ of the primary beam, where $\tan\beta = y'_0/x'_0$. Then power is fed back by the beam into the breakup mode at a rate proportional to the component of $\mathbf{r}$ in the direction β, i.e., $\mathbf{r}\cdot\hat{\mathbf{r}}'_0 = (R_{12}\, x'^2_0 + R_{34}\, y'^2_0)/r'_0$. Thus it is clearly advantageous for R_{12} and R_{34} to be of opposite sign and in fact at $R_{12}/R_{34} = -\tan^2\beta$, $\mathbf{r}$ is orthogonal to $\mathbf{r}'_0$, so that regenerative BBU will not occur. This analysis ignores the fact that the transverse modes occur as orthogonal pairs and would only be useful if one of the pair were dominant for some reason. It also assumes that the beam does not couple the orthogonal modes, which is generally true in superconducting structures, where the separation of the modes is typically of order 10^4 bandwidths.

In the more general case where the orthogonal modes have roughly equal Q values, complete damping of the second mode, oriented at (90° + β) to the horizontal plane would require $R_{34}/R_{21} = -\tan^2\beta$. Obviously both modes cannot be completely damped simultaneously unless $\beta = 45°$. In general the best compromise for the two modes is $R_{12} = -R_{34}$ giving $\mathbf{r}\cdot\hat{\mathbf{r}}'_0 = R_{12}\, r' \cos 2\beta$. This is illustrated in Fig. 5(a). This condition therefore increases the BBU starting current by a factor $|1/\cos 2\beta|$ compared with the case $R_{12} = R_{34}$.

It is worth noting that if the structures are designed in such a way that the transverse modes are oriented at 45° to the orbital bending plane, BBU in the first orbit can be eliminated entirely in principle. This simple requirement of the structure design together with beam optical reflection provides an economical method of achieving high currents. To achieve the optimum conditions $R_{12} \simeq -R_{34}$ (where the exact equality holds only if the Q values of the orthogonal modes are equal) is not difficult and does not require the magnifications in the two planes to be exactly equal and opposite.

Suppose for instance that one has the situation shown by the vector $\mathbf{r}$ in Fig. 5(b) where $R_{12} \neq -R_{34}$, i.e., $\beta \neq \gamma$. By a slight adjustment of one of the orbit quadrupole strengths by an amount ΔQ, one can modify R_{12} and R_{34} to be $(R_{12} + k\, \Delta Q\, X_p/M_x)$ and $(R_{34} - k\, \Delta Q\, X_p/M_y)$ respectively, where k is a constant. Thus the tip of the vector $\mathbf{r}$ can be made to trace the straight dashed line shown in the figure until $\gamma = \beta$. This apparent rotation of the vector $\mathbf{r}$ has been demonstrated both using TRANSPORT and in practice, on the first orbit of the SCR. A change of the strength of the second quadrupole in the orbit by

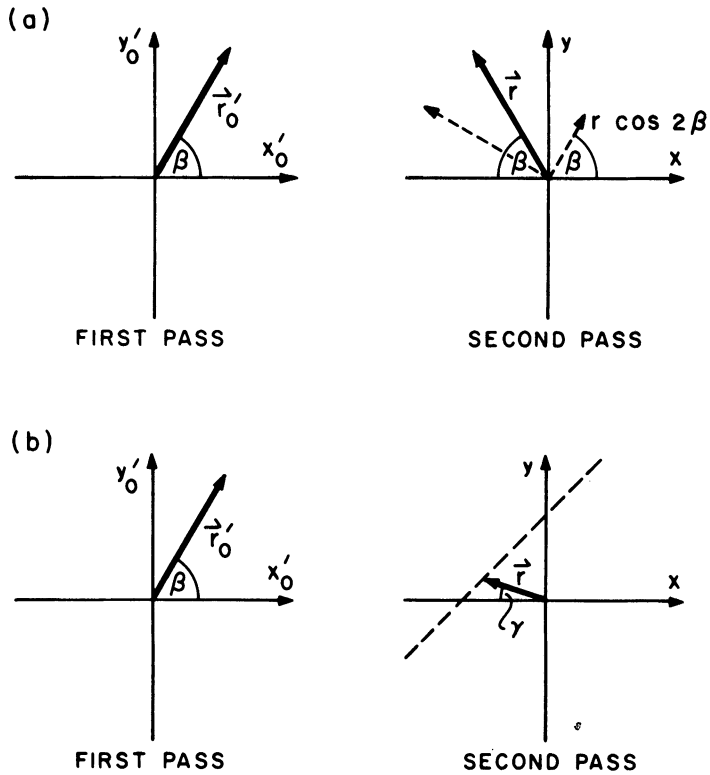

FIGURE 5 (a) Beam reflection with $R_{12} = -R_{34}$. The component of $\mathbf{r}$ in the direction of $\mathbf{r}'_0$ is $r \cos 2\beta$.
(b) Rotation of the displacement $\mathbf{r}$ by adjusting a single quadrupole. The tip of the vector $\mathbf{r}$ follows the dashed line.

only 1% is sufficient to rotate $\mathbf{r}$ by 90°. This was achieved using the orbit configuration described earlier ($M_x = -0.44$, $M_y = 0.51$).

3.4 Beam Rotation

Pure "rotation" of the beam so that the displacement on the second pass is always orthogonal to the deflection which causes it during the first pass, as shown in Fig. 6, would clearly eliminate BBU altogether for 2-pass operation, provided coupling between the orthogonal modes is negligible, and whatever their orientation. This would require an orbit matrix of the form

$$\begin{bmatrix} & & M & \Delta L \\ & & C & X/M \\ -M & -\Delta L & & \\ -C & -X/M & & \end{bmatrix},$$

where ΔL is given by formula (3) or (5) for R_{12}. Such a matrix is not difficult to realize in principle and practical ways of achieving it are discussed below.

Assuming that all interactions between the first- and second-pass beams can be eliminated, the

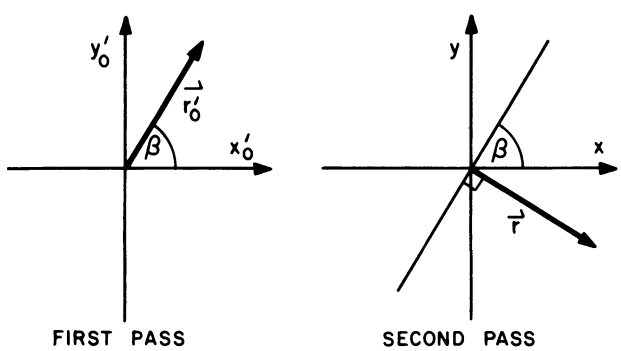

FIGURE 6 90° Beam rotation $(x'_0, y'_0) \rightarrow (-y, x)$.

question again arises as to the optimum optics for subsequent orbits. Further rotation of the beam would not be desirable, since then interaction could occur between a higher-pass beam and the first-pass beam. Any mixing of the two planes even by different magnifications would have this effect. Subsequent orbit matrices should therefore be as described previously. BBU could then occur between the second-pass beam and subsequent passes, but the effective injection energy would have been increased to that of the second-pass beam. The gain in BBU starting current due to this effect would therefore be at least a factor of 2, but more probably an order of magnitude if breakup occurred at the injection end of the linac. This would be the real gain from beam rotation in the first orbit.

4 PRACTICAL REALIZATION OF BEAM ROTATION

4.1 Beam Rotating Devices

(a) *Solenoids* The beam-transport device that immediately comes to mind in connection with rotation is the solenoid. It is, however, unsuitable for this particular application, as is shown below.

The transport matrix for a solenoid may be written as the product of a rotation matrix and a particular thick-lens matrix. For the case of rotation by 90° it is

$$\begin{bmatrix} & & 1 & \\ & & & 1 \\ -1 & & & \\ & -1 & & \end{bmatrix} \begin{bmatrix} & \frac{1}{K} & & \\ -K & & & \frac{1}{K} \\ & & & \\ & & -K & \end{bmatrix} = \begin{bmatrix} & & & \frac{1}{K} \\ & & -K & \\ & -\frac{1}{K} & & \\ K & & & \end{bmatrix}$$

where $K = B_0/2B\rho$, B_0 is the field inside the solenoid and $B\rho$ is the rigidity of the beam. For this 90° rotation, the length of the solenoid is $l = \pi/2K$.

The problem with this matrix is that it interchanges displacement with deflection, which, although it can be corrected by the remainder of the orbit optics, has unfortunate consequences for the physical length of the solenoid. To take the Stanford SCR as an example, the recirculation system is designed to operate with a maximum beam size in the first orbit of ±2.5 mm and maximum angular spread of ±0.1 mr at 120 MeV. In order that the beam leaving the solenoid should not exceed these limits, the value of K must be given by $K^{-1} \simeq 25$ m. This implies a solenoid length of approximately 39 m and a field of 320 G, quite impractical values. Furthermore, for any solenoid producing 90° rotation, the product of length and field would remain the same, implying at best a very bulky and expensive device, either conventional or superconducting. If the solenoid could be made with a field of 20 kG and length 0.63 m, it would produce a highly divergent beam requiring correction by at least a quadrupole triplet. It would be better to split the solenoid into 3 parts, rotating the beam by 22.5°, 45° and 22.5° respectively and separated by drift spaces, each of length 2/K. This would produce a (negative) unit matrix with a 90° rotation but still each solenoid would hardly be a practical device.

b) Rotation by Reflection Beam reflection with all matrix elements in the two planes equal and opposite is commonly used to rotate the plane of dispersion of a beam by 90°[10,11] by setting the reflecting plane at 45° to the x- or y-axis. This arrangement is adequate for operating "energy-loss" spectrometers for instance. It does not, however, give a true rotation, but only a pseudo-rotation of the general form

$$\begin{bmatrix} & & 1 & \Delta L \\ & & & 1 \\ 1 & \Delta L & & \\ & 1 & & \end{bmatrix}$$

where ΔL is determined by the details of the optics. This is not suitable for the present purpose. A true rotation can be obtained by combining this rotated reflector with a second reflector oriented normally. The resulting transport matrix is then

$$\begin{bmatrix} 1 & \Delta L & & \\ & 1 & & \\ & & -1 & -\Delta L \\ & & & -1 \end{bmatrix} \times \begin{bmatrix} & & 1 & \Delta L \\ & & & 1 \\ 1 & \Delta L & & \\ & 1 & & \end{bmatrix}$$

$$= \begin{bmatrix} & & 1 & 2\Delta L \\ & & & 1 \\ -1 & -2\Delta L & & \\ & -1 & & \end{bmatrix}$$

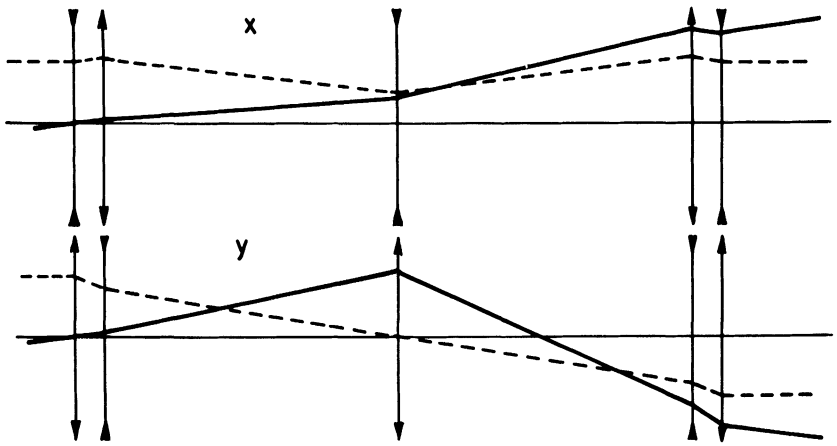

FIGURE 7 Beam reflector using 5 quadrupoles.

This is the form of matrix required for true beam rotation. It can be realized in a recirculation system by a single reflector at 45°; the second inversion is performed by the orbit itself.

4.2 Practical Beam Reflectors

Beam transport elements which produce reflections about a mirror plane with optical length equal to their physical length are well known. The basic arrangement consists of 5 quadrupoles. Its optical mode is illustrated in Fig. 7. Similar arrangements may be devised with zero optical length.

A simple reflector, although with a limited range of application, consisting of three approximately equal-length bending magnets with parallel pole faces is shown in Fig. 8.

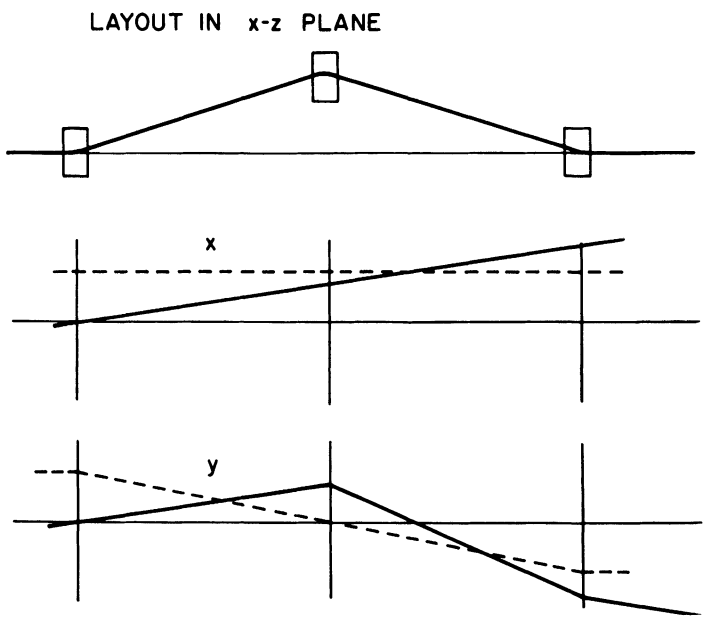

FIGURE 8 Beam reflector using 3 bending magnets.

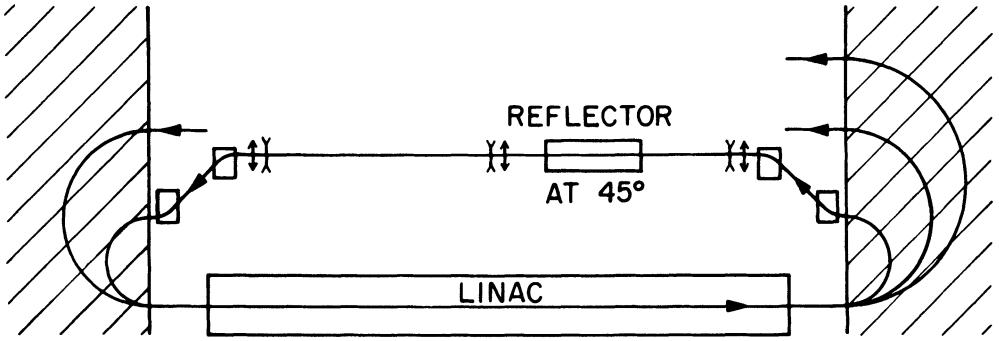

FIGURE 9 Possible layout for the first orbit of a recirculating accelerator incorporating a reflector installed at 45° to the bend plane in a region of zero dispersion. Quadrupole pairs sufficient to produce true rotation of the beam at the linac and diagonal matrix focusing are shown.

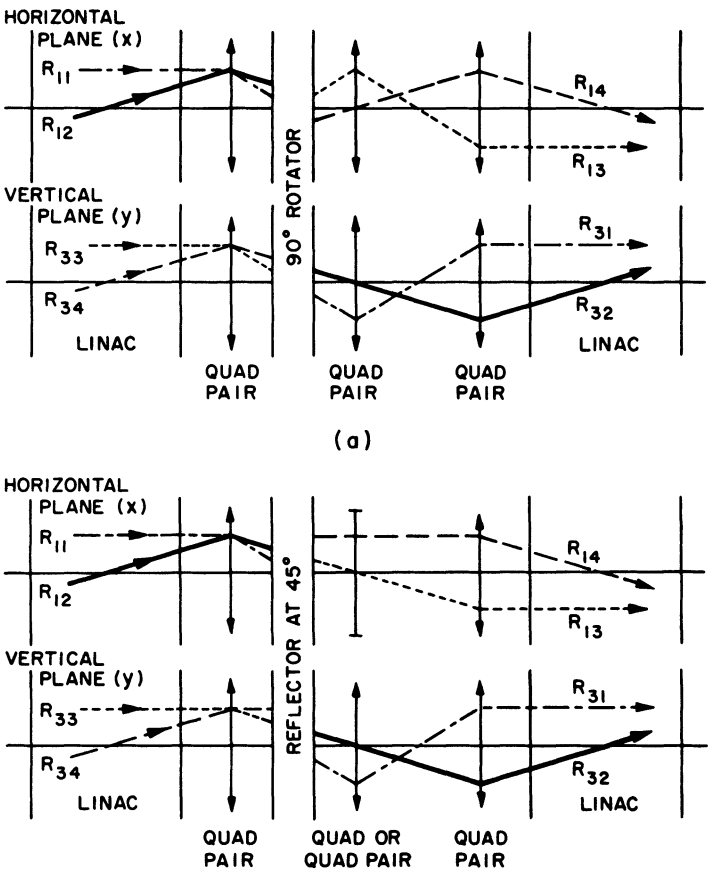

FIGURE 10 Incorporation of (a) a 90° rotator and (b) a pseudo-rotator (reflector at 45°) into the orbit optics of a recirculating accelerator. Dispersive elements are omitted.

4.3 Incorporation of Rotation Into Orbit Optics

It has already been pointed out that rotation of the beam is desirable only in the first orbit of a recirculating accelerator and for this reason it is undesirable to install a rotator on the linac axis where all beams would be affected to some extent. The obvious site therefore for the rotator is the "backleg" of the first orbit. In this region the beam is usually dispersed, so that a prerequisite for the rotation is that this dispersion first be removed unless it is of such a magnitude that vertical dispersion of the beam would not be troublesome. A first-order design for a race track microtron or recyclotron which would achieve this end, incorporate rotation and allow diagonal matrix focusing, is shown in Fig. 9. Details would depend on the quality of the first-pass beam and permissible degradation of this quality in subsequent passes.

Finally, ignoring the problems of dispersion and the effects of the 180° bends, Fig. 10 shows how (a) a 90° rotator and (b) a reflector mounted at 45° may be incorporated into the complete orbit optics to produce pure rotation in both cases, with diagonal matrices. The position of the rotator or reflector is quite arbitrary. The arrangement 10 (b) could in fact provide rotation of the first orbit beam with diagonal matrix conditions, with the minimum number of 10 quadrupoles.

5 CONCLUSION

It has been shown that from the point of view of BBU, the desirable properties of the orbit optics in a recirculating accelerator are in order of importance as follows:

First orbit:

(a) point-to-point focusing at a position about one-third the length of the linac from the injection end and preferably also near each end of the linac;
(b) magnification $\simeq \pm(E_A/E_B)^{1/2}$, (opposite signs in two planes)
(c) approximately diagonal matrix;
(d) reflection mode ($M_x = -M_y$, $R_{12} = -R_{34}$);
(e) beam rotation.

Subsequent orbits:

(f) point-to-point focusing as for first orbit;
(g) magnification $\simeq \pm(E_M/E_N)^{1/2}$ in both planes;
(h) approximately diagonal matrix.

Of these items, the effectiveness of (a), (d) and (f) have been demonstrated on the Stanford SCR. The remaining items indicate that up to two orders of magnitude increase in BBU starting currents can be achieved in this machine by beam optical methods.

6 ACKNOWLEDGEMENTS

The authors are grateful to their colleagues in the Stanford superconducting accelerator group for their support of this study and for assistance with the experimental measurements. They are particularly indebted to Prof. H.A. Schwettman and Mr. A.M. Vetter for some illuminating discussions on the mechanism of beam breakup. Prof. A.O. Hanson of the University of Illinois also provided some useful insight.

APPENDIX

Orbit Matrix Element for a Travelling-Wave Linac

Using the notation of Fig. 1 and section 3, the transport matrix for a traveling-wave structure[7] is

$$\alpha_A(L) = \begin{bmatrix} 1 & L_A \ln(1/X_A) \\ 0 & X_A \end{bmatrix}$$

Hence:

$$\frac{R_{12}}{E_A + E} = \frac{L_0}{E_0}\left[\frac{1}{M}\ln(1/X_B) - M\ln(1/X_A) - \frac{E_B}{E_0} CL_0 \ln(1/X_A)\ln(1/X_B)\right]$$

The Power series expansion for R_{12} is

$$R_{12} = L\left[\frac{X_p}{M} - M\right] + \frac{L^2}{L_0}\left[\frac{E_0}{2E_A}\left(\frac{X_p}{M} - M\right) + \frac{E_0}{2E_A}(1 - X_p)\frac{X_p}{M} - CL_0\right] + \frac{L^3}{L_0^2}$$

$$\times\left[-\frac{E_0^2}{6R_A^2}\left(\frac{X_p}{M}-M\right)+\frac{E_0^2}{6E_A^2}\,(1-2X_p)\right.$$
$$\left.\times(1-X_p)\,\frac{X_p}{M}-\frac{E_0}{2E_A}\,(1-X_p)\,CL_0\right]+\ldots$$

REFERENCES

1. R.S. Livingston et al., The Role of Electron Accelerators in U.S. Medium Energy Nuclear Science, ORNL Report ORNL/PPA-77/4 (1977).
2. C.M. Lyneis et al., *IEEE Trans. Nucl. Sci.* **NS-26**, 3246 (1979).
3. P. Sargent, Conf. on the Future Possibilities for Electron Accelerators, Charlottesville, Virginia, January 1979.
4. P. Axel et al., *IEEE Trans. Nucl. Sci.* **NS-26**, 3143 (1979).
5. A.M. Vetter, C.M. Lyneis, and H.A. Schwettman, *IEEE Trans. Nucl. Sci.* **NS-26**, 3757 (1979).
6. H. Herminghaus, Conf. on the Future Possibilities for Electron Accelerators Charlottesville, Virginia, January 1979.
7. K.L. Brown, D.C. Carey, Ch. Iselin, and F. Rothacker, SLAC-91, February (1974).
8. Another common notation is $R_{12} = < x|\, x'_0 >$.
9. E.E. Chambers, Proc of the 1968 Summer Study on Superconducting Devices and Accelerators, **BNL** 50155, 1968, and HEPL TN-68-17, Stanford, (1968).
10. S.B. Kowalski and H.A. Enge, Proc 4th International Conf. on Magnet Technology, New York 1972, USAEC-Report No. CONF-720908, (1972).
11. Th. Walcher, R. Frey, H-D Gräf, E. Spamer, and H. Theissen, Darmstadt Preprint IKDA 77/26 (1977).